Calculation for the Heating and Safe Operation Time of YKK Series High-voltage Motors in Starting Process

Yunyan Xia[*], Dawei Meng and Yongming Xu

College of Electrical & Electronic Engineering, Harbin University of Science and Technology, Heilongjiang, Harbin, 150080, P. R. China

Abstract: In order to analyze the heating and cooling conditions of high voltage motors of YKK series in starting process, the starting characteristics and ventilation systems are calculated. The starting characteristics calculation method is improved and compared with the static characteristic, dynamic characteristics come to more consistent with the actual situation. The calculation result of heating is more accurate according to the calculation of dynamic characteristics. A wind-resistance network model is built combined with the motor cooling structure to calculate the distribution of air flow in the motor. The locked-rotor safety running time in starting process is calculated based on the accurate calculation of heating and cooling condition. The result is more close to the experiment and it has an important significance to the design and improvement of YKK series high voltage motor.

Keywords: Starting characteristics, wind-resistance network, safety running time.

1. INTRODUCTION

High voltage motors of YKK series are widely used in power system, and the starting process has a great impact to power grid and other equipment comparing with other motors [1]. One of the problems which the production and design departments especially concerned about is that the locked-rotor condition and motor temperature rise of starting process directly affect the service life. At present, the method of temperature rise calculation in the engineering generally uses the steady characteristics curve instead of the starting current and torque variation, then, the actual safety running time of the motor is got by the safe operation time of adiabatic calculation multiplied by the corresponding coefficient [2]. The computational accuracy is greatly reduced although the method is simply.

In this paper, starting characteristics is calculated based on the dynamic equations of three-phase induction motor, and the accuracy of heating calculation is improved. Aiming at the specific structural, the model is built with the method of wind-resistance network, the flow and movement speed of fluid is solved. On the base of calculating the heat generation and heat dissipation of the motor in each time period, the locked-rotor safety running time is calculated and the average temperature rise of stator and rotor can be obtained by the cumulative temperature rise.

2. STATOR AND ROTOR HEAT CALCULATION OF HIGH VOLTAGE MOTORS

Starting process is a transient process, current and torque will change with the increasing speed, and the heat generated

by the currents is also changing. In order to calculate accurately the starting current and torque of the motor, dynamic equation (1) is established to calculate the motor starting characteristics considering the magnetic flux changes of starting process [3-5]. A 690kW, 6kV motor of YKK series is calculated [6], the starting characteristics result is shown in Fig. (**1**).

$$
P\begin{bmatrix} i_{M1} \\ i_{T1} \\ i_{M2} \\ i_{T2} \end{bmatrix} = \begin{bmatrix} X_{ss} & 0 & X_m & 0 \\ 0 & X_{ss} & 0 & X_m \\ X_m & 0 & X_{rr} & 0 \\ 0 & X_m & 0 & X_{rr} \end{bmatrix}^{-1} \left\{ \begin{bmatrix} u_{M1} \\ u_{T1} \\ 0 \\ 0 \end{bmatrix} \right.
$$
$$
+ \begin{bmatrix} -r_1 & X_{ss} & 0 & X_m \\ -X_{ss} & -r_1 & -X_m & 0 \\ 0 & X_m & -r_2 & X_{rr} \\ -X_m & 0 & -X_{rr} & -r_2 \end{bmatrix} \begin{bmatrix} i_{M1} \\ i_{T1} \\ i_{M2} \\ i_{T2} \end{bmatrix}
$$
$$
+ \omega \begin{bmatrix} 0 & 0 & 0 & 0 \\ 0 & 0 & 0 & 0 \\ 0 & -X_m & 0 & -X_{rr} \\ X_m & 0 & X_{rr} & 0 \end{bmatrix} \begin{bmatrix} i_{M1} \\ i_{T1} \\ i_{M2} \\ i_{T2} \end{bmatrix} \right\}
$$

(1)

Where r_1, r_2 are per phase resistances of the stator and the rotor, u_{M1}, u_{T1} are the two-phase voltage of the stator, i_{M1}, i_{T1}, i_{M2}, i_{T2} are the two-phase current of the stator and the rotor, P is the differential operator, ω is the speed of the rotor angle, X_{ss}, X_{rr}, X_m are the self reactance of the stator and the rotor and the mutual reactance of the stator and the rotor.

It is easy to see that the strong pulsating component is included in the torque and current of dynamic characteristic curves in low-speed section. That is because the stator current has low frequency component and non-periodic compo-

*Address correspondence to this author at the College of Electrical & Electronic Engineering, Harbin University of Science and Technology, 150080 P. R. China; Tel: 15045100584; E-mail: yunyan_x@163.com
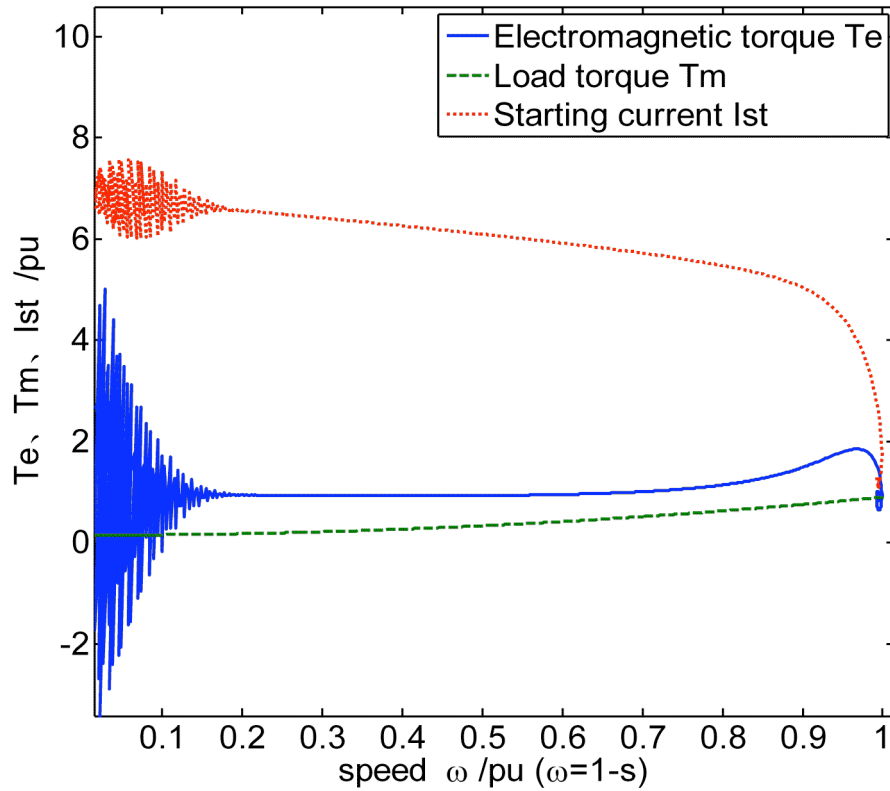
Fig. (1). Dynamic characteristics curve.

nent in addition to the fundamental frequency alternating component. Since the non-periodic component produces static magnetic field and the three-phase fundamental current produces the rotating magnetic field at synchronous speed, the frequency of the induced current in the rotor bar is $(1-s)f_1$ and sf_1. The stator current and rotor current whose frequency is sf_1 produce a rotating magnetic field which is a relatively stationary in space, and produce one-direction torque. The static magnetic field produced by the non-periodic stator current and rotor current at the frequency of $(1-s)f_1$ interacts with the synchronous rotating magnetic field, which produces an alternating electromagnetic torque. The alternating torque component appears when the transient is taken into account. It can decrease to zero with the attenuation of the non-periodic current component [7]. The starting process of motor is a transient process, dynamic characteristic curve is more in line with the actual situation.

Calculates the calorific on the basis of the starting characteristics, in the starting process the stator current generate heat, the stator winding average temperature rise in time Δt can be expressed as follows:

$$\Delta\theta = \frac{j_s^2 \cdot \rho \cdot \Delta t}{C_s \cdot \rho_s} \tag{2}$$

Where j_s is the current density of stator winding, A/m2; ρ is the stator winding resistivity,$\Omega \cdot$m,C_s is the specific heat of stator winding, J/(kg °C), ρ_S is the stator winding density,kg/m3.

Because the stator winding resistivity significantly increases with temperature, assume the resistance temperature

coefficient is α at 15°C, adiabatic temperature rise when the time is t can be expressed as follows:

$$\theta_{s1} = \frac{A}{B} e^{j_s^2 \cdot B \cdot t} - \frac{A}{B} \tag{3}$$

Where A=ρ [1+(θ_0-15)α] / $\rho_s C_s$, θ_0 is the environment temperature, B= $\rho\alpha$ / $\rho_s C_s$.

When the slip changes from s_1 to s_2 in the starting process, the rotor winding heat is expressed as follows[8]:

$$Q = \frac{GD^2}{4} \omega_1^2 \int_{s_2}^{s_1} \frac{s}{1 - \frac{M_m}{Me}} ds \tag{4}$$

Where M_m is the load torque, M_e is the electromagnetic torque.

The equivalent resistance of rotor bar R_B in the starting process and the equivalent resistance of end ring R_k are expressed as follows:

$$R_B = \frac{R_{BN} + R_{BS}}{R_N + R_S} \quad R_K = \frac{R_{KN} + R_{KS}}{R_N + R_S} \tag{5}$$

Where R_{BN}, R_{BS}, R_{KN} and R_{KS} are rotor bar and end ring resistances when the motor is in the rated operation and locked rotor, R_N and R_S are rotor resistances when the motor is in the rated operation and locked rotor ($R_N = R_{BN} + R_{KN}$, $R_S = R_{BS} + R_{KS}$).

The calorific value of rotor bar Q_B and the calorific value of end ring Q_K are expressed as follows:
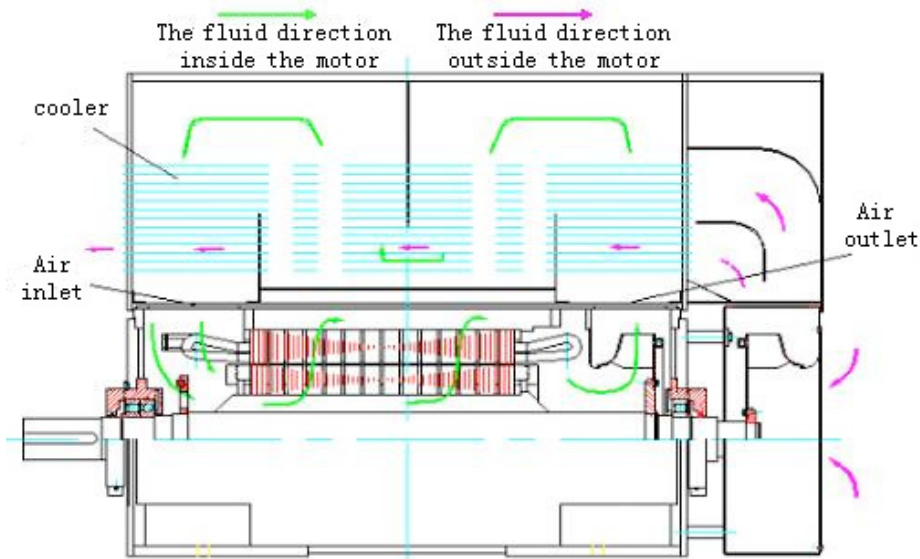
Fig. (2). The graph of motor ventilation system.
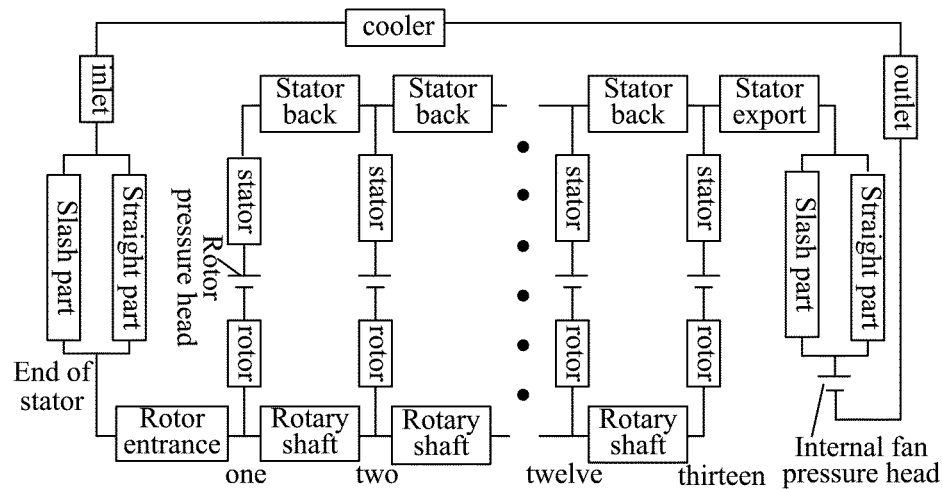
Fig. (3). The motor graph of windage resistance network.

$$Q_B = R_B \cdot Q \quad Q_K = R_K \cdot Q \tag{6}$$

3. HEAT DISSIPATION CALCULATION OF HIGH-VOLTAGE MOTOR

3.1. Establishment and Calculation of the Wind Network

Generally, inside and outside air-air cooling structure is used in YKK series motors. Axial and radial mixing ventilation structure is used in the prototype. Ventilation structure and the flow condition of the fluid are shown in Fig. (**2**).

In order to calculate accurately the heat dissipation of the motor, the distribution of air volume in the motor and the wind speed should be known. The air volume is solved by the equivalent airflow with lumped parameters which makes the complex aerodynamic problems translated into the solving of equivalent airflow consisting of wind resistance and wind pressure source. Because air gap of the stator and rotor is very small and wind resistance is very big, cooling air into the air gap can be ignored. Fig. (**3**) is the equivalent wind network of the selected prototype.

There is a wind resistance in the ventilated place, the wind resistance of wind path inside the motor is calculated as follows:

$$Z = \xi \cdot \frac{\rho}{2} \cdot \frac{|Q_f|}{S^2} \tag{7}$$

Where ξ is the local resistance coefficient, ρ is the fluid density, Q_f is the fluid flow, S is the flow area.

The wind resistance of the radial wind path includes entrance wind resistance, route wind resistance and export wind resistance. And the route resistance coefficient of the gear and yoke of stator is calculated as follows:

$$\xi_s = \frac{0.3164}{\sqrt[4]{R_e}} \cdot \frac{l}{d} \tag{8}$$

The coefficient of local resistance in the rotor radial spinning wind path is calculated as follows:

$$\xi_r = \frac{0.3164}{\sqrt[4]{R_e}} \cdot \frac{l}{d} \left(1 + 0.52 R_e^{0.25} \left(\frac{\omega d}{\upsilon} \right)^{0.58} \right) \tag{9}$$
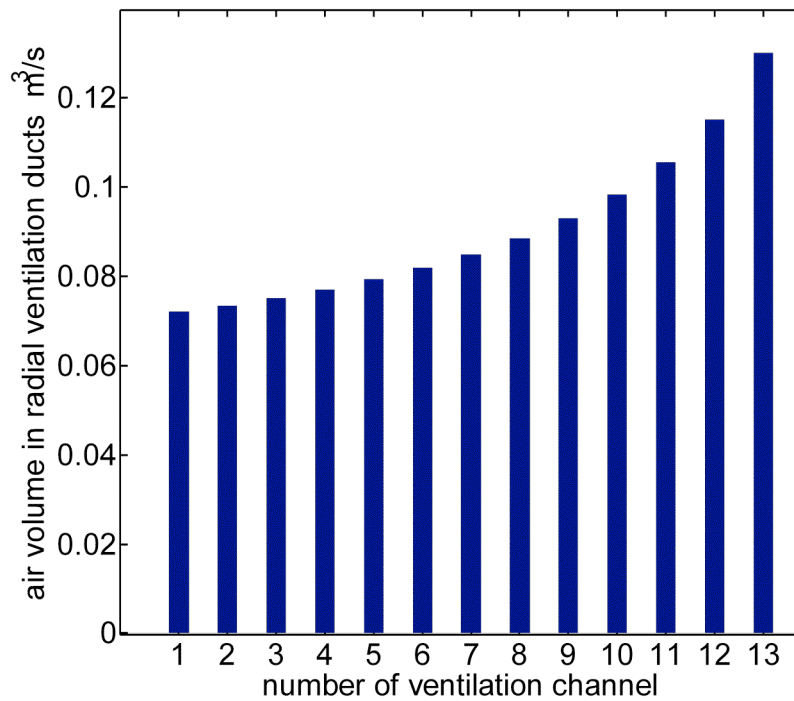
Fig. (4). The air distribution in radial ventilation duct.

Where l and d are respectively for the length and equivalent diameter of the fluid channel, $R_e = \upsilon l / d$ is the Reynolds number, υ is the fluid relative speed.

According to the calculated wind resistance the voltage drop on the wind resistance Z is calculated as follows:

$$H = Z \cdot Q_f \qquad (10)$$

The wind network of the motor is a complex nonlinear network. In the starting process, the flow state of fluid in the motor changes with different rotate speeds. When the motor is in the steady state, the cooling air will enter a stable circulatory state. The wind network of the motor is solved by the network topological method. The initial value is given and iterative calculation is adopted [9]. At last, the wind resistance of the wind network is modified according to the changed wind volume in the motor until the wind path to achieve a stable circulatory state. Reynolds number R_e can be calculated on the condition that wind speed is known, and then the fluid movement state at the calculation moment can be determined. And the wind resistance which is the function of the Reynolds number can be also calculated accurately [10].

The fluid flow of the motor which is 1.1748m3/s is obtained by calculating the selected prototype. Fig. (**4**) is the air volume distribution of 13 wind paths from air inlet to air outlet.

The figure shows that the distribution of air flow from 1 radial ventilation duct to 13 radial ventilation duct increases gradually. Because the axial cooling air flow is great, the velocity is high and the motion inertial is large at the entrance to the rotor axis, the flow which comes into 1 radial ventilation duct is small. The air flow that comes into the radial direction increases gradually with the speed of air axis decreasing. Calculation results correspond with the air movement rules.

Path of the flow from 1 ventilation duct to 13 ventilation duct is different in the rotor axial direction. The flow of 1 ventilation duct is through the rotor bracket of the first segment iron core. The flow of 2 ventilation duct is through the rotor brackets of the first segment iron core and the second segment iron core. So the flow of 13 ventilation duct is almost through the entire rotor brackets. With the number of ventilation duct increasing, the fluid temperature which is at the entrance to the ventilation duct of the rotor radial direction increases gradually. Though the cooling air flow of 1 ventilation duct is the smallest, the temperature of 1 ventilation duct which comes into the radial ventilation groove of the rotor is also the lowest. Fluid flow of 13 ventilation duct is the largest and the temperature of 13 ventilation duct which comes into the radial ventilation duct of the rotor is also the highest. Therefore, the heat taken away by the cooling air of each ventilation duct is close to the same, which is beneficial to the temperature balance along the axial direction and corresponds with the design goal of motor ventilation cooling system [11].

The flowing air of ventilation duct is influenced by the ventilation slot board of the stator and rotor. Because orifice areas of the stator tooth and the yoke are different, the cooling air flow rate of the tooth and the yoke is also different. Fig. (**5**) is the tooth and yoke average wind speed of the stator and rotor.

3.2. The Heat Dissipation Model of the Motor

The calculation of the motor heat dissipation is based on the heat dissipation coefficient of the motor inner surface. When the fluid motion speed in the motor is known, the calculation accuracy of heat dissipation coefficient can be improved. The heat dissipation coefficient of the motor ventilation groove inner surface is calculated as the following formula [12].
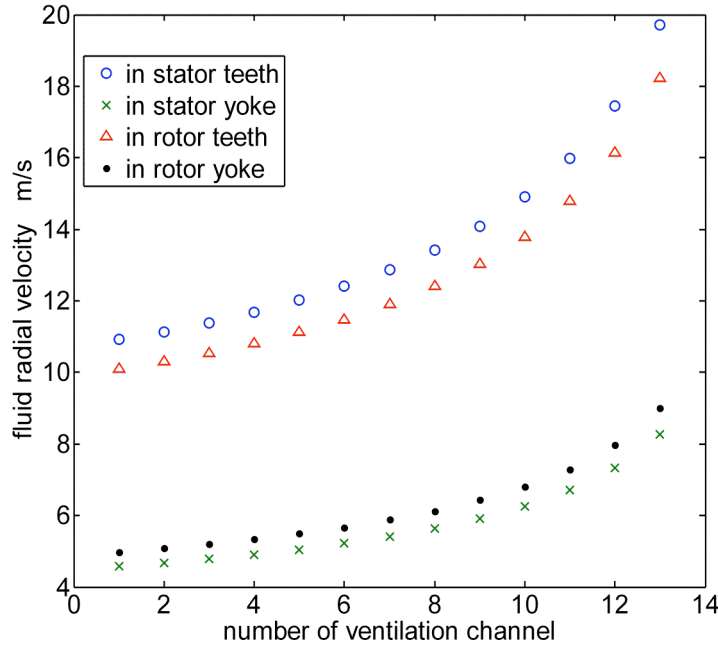
Fig. (5). The air distribution in radial ventilation duct.

$$\alpha = 0.023 R_e^{0.8} P_r^{0.4} \varepsilon \frac{\lambda}{d} \qquad (11)$$

Where P_r is the Prandtl constant, ε is the correction coefficient and λ is the coefficient of thermal conductivity.

For the motor of Hybrid ventilation structure, heat between the stator windings and core is transferred by the stator insulation and heat between the rotor bar and core is transferred by conduction. In the ventilation channel and the end, the heat of stator winding and the rotor bar is transferred by convection with air. The heat emission of stator winding when time is t is expressed as follows [13]:

$$Q_1 = \left(\frac{\Delta\theta_{s1}}{R_{s1}} + \frac{\Delta\theta_{s2}}{R_{S2}} + \frac{\Delta\theta_{s3}}{R_{S3}} \right) \cdot t \qquad (12)$$

Where R_{s1}, R_{s2}, R_{s3} are thermal resistances between the stator winding and iron core, the air at the end of stator, and air in the radial ventilation channel, $\Delta\theta_{s1}$, $\Delta\theta_{s2}$, $\Delta\theta_{s3}$ are the temperature differences between the stator winding and iron core, the air at the end of stator, and air in the radial ventilation channel.

Actual temperature rise is expressed when the time is t as follows:

$$\theta_s = \theta_{S1} - \frac{Q_1}{C_s M_s} \qquad (13)$$

And the thermal resistance of rotor bar and the heat emission Q_{B1} can be calculated when the slip changes from S_1 to S_2 in time t_1. The end ring dissipates the heat by convection with the air, so the heat which is transferred between the rotor bar and the end ring can not be considered. According to the thermal resistance of the end ring and the heat emission of the end ring Q_{K1} in time t_1 can be calculated. Then the actual temperature rise of the end ring in time t_1 can be calculated.

4. CALCULATION METHOD AND CALCULATION RESULTS OF THE TEMPERATURE RISE AND THE SAFE OPERATION TIME

This paper solves the dynamic equation of the motor by the improved algorithm and solves the wind network which is established according to the motor structure by the network topologic method. Then the flow distribution of cooling air can be determined and the heat dissipation can be accurately calculated, which has great significance for accurately calculating the safe operation time of the motor. The motor starts with the electromagnetic transition. In the starting process, the calculation step length is 20 ms and the heat that the motor generates and the heat dissipation are calculated in each step length, which can improve the calculation accuracy and ensure the calculation speed.

Generally, the initial value in the starting process is zero. According to the initial value, the starting characteristics of the motor can be calculated and then the stator current density, the electromagnetic torque and the speed can be obtained after a step length. The adiabatic temperature rise of the stator winding can be calculated according to the formula (3). Then the temperature difference between the winding and the surrounding environment is brought into the formula (12) and the heat dissipation of the winding can be calculated. According to the changing slip, the heat that the motor generates and the heat dissipation of the rotor bar and the end ring can be calculated in a time step length. Also, the temperature rise also can be obtained according to the heat and heat dissipation of the stator and rotor windings in the step length. The heat dissipation rate of the stator winding, rotor bar and the end ring can be calculated according to the heat dissipation. At last, the safe operation time in the step length can be calculated when the rotor is locked.

When the rotor is locked, the resistance of rotor bar is bigger than the normal operation because of the skin effect at the locked-rotor condition. The skin effect coefficient K_w is
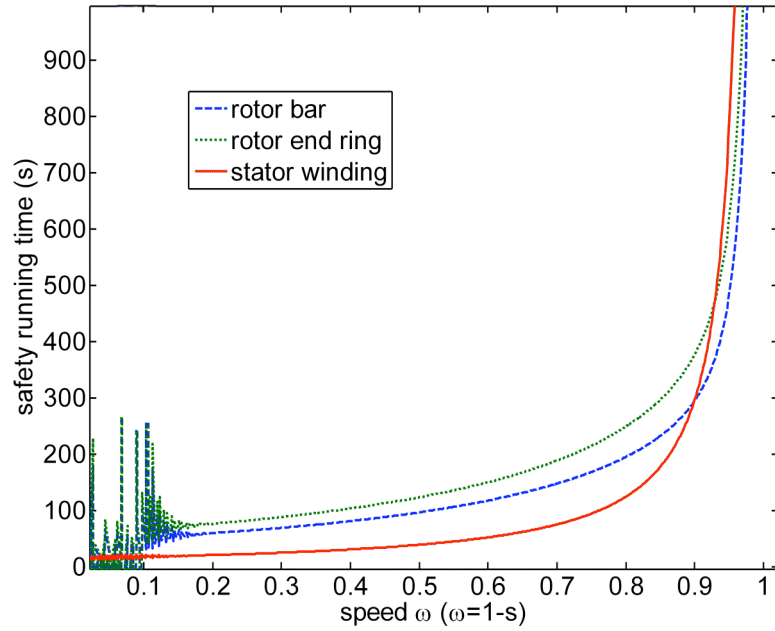
Fig. (6). Allowed locked-rotor running time.

the ratio of the rotor resistance which the alternating frequency leads to and the bar resistance. K_w can be calculated as the following formula.

$$K_w = \frac{P_1 - P_{Cu1} \cdot I^2 - P_{Fe1} - P_{Fe2} - P_s}{P_{Cu} \cdot I^2} \qquad (14)$$

Where P_1 is the input power of the motor when the motor is in the stall state, P_{Cu1} is the stator copper consumption of the motor, P_{Fe1}, P_{Fe2} is the iron consumption of the stator and rotor, P_s is the stray loss of the motor, I is the starting current multiple when the motor is in the stall state and P_{Cu} is the rotor copper consumption which is obtained by the electrical performance test of the motor.

The safe operation time of the stator and rotor when the motor is in the starting process can be calculated as following three formulas.

$$t_s = \frac{\ln(\theta_1 B + A) - \ln A}{j_s^2 B}$$

$$t_B = \frac{\theta_{BS} \cdot C_B \cdot M_B}{P_{Cu2} \cdot R_B \cdot K_w - q_b} \qquad (15)$$

$$t_K = \frac{\theta_{KS} \cdot C_K \cdot M_K}{P_{Cu2} \cdot R_K \cdot K_w - q_r}$$

Where t_s, t_b, t_k are the safe operation times of the stator winding, rotor bar and the end ring, θ_1, θ_{BS}, θ_{KS} are the limiting temperature rise that the stator and rotor allows, R_B, R_K is the proportion, P_{Cu2} is the rotor copper consumption and q_b, q_r is the heat dissipation rate of the bar and the end ring in the calculating step length.

So far the starting characteristics and the calculation of the stall time end in a step length. The result is considered as the initial value of the next step and the above process is repeated. Temperature rise of each step length is accumulated and the average temperature rise of the motor windings can be ob-

tained. The starting characteristics calculation ends until the motor current and the electromagnetic torque reach stable values. Finally, the motor comes into the stable operation.

When the winding temperature rise is calculated, in order to obtain the temperature difference between the windings and the iron core, the temperature rise of the iron core should be calculated. Besides the conduction heat, iron cores of the stator and the rotor have itself consumption. The iron core convects and dissipates heat with the air through the ventilating duct, the stator back and the internal diameter of the rotor. The temperature rise can be calculated by the heat relationship. The heat which is taken away by the cooling air in the ventilation duct and the stator back can be got by the heat dissipation calculation of the motor. According to the distribution of the cooling air in each part of the motor, the temperature rise value of the cooling air can be obtained, which avoids the boundary problem in the solving temperature field and makes the calculation more simple and accurate.

Fig. (6) is the calculation results of the safe operation time for the stator and rotor windings of the prototype. It shows that at the beginning of starting process, the locked-rotor safety running time is not stable. As we can know from the paper front, at the beginning of starting process, current and electromagnetic torque have great vibration components, so the safety running time of the motor has fluctuation. The locked-rotor safety running time is short when the motor works at low speed. The safety running time of the winding is about 20 seconds at the beginning step, and the time increases with the revolving speed, while, when the revolving speed reaches the level, The motor can achieve safe operation state.

5. CONCLUSION

Dynamic equations and wind network model of the medium-sized high-voltage motors are built, also starting characteristics and specific fluid distribution is calculated. The paper calculates the ventilation and heating of the motor

more accurately, so the wind distribution of the mixing ventilation structure and lock-rotor safety running time of the starting process are calculated. The calculation results close to the experimental results, it provides evidences to the motor design, and the calculation method is simple. When we calculate motors of different structures, just need to modify the original parameters. It is suitable for engineering applications.

CONFLICT OF INTEREST

The authors confirm that this article content has no conflicts of interest.

ACKNOWLEDGEMENTS

REFERENCES

[1]　J. B. Wen, and G. H. Wang, "Calculation and analysis of 3D temperature fields of medium size high voltage asynchronous motor based on coupled field", *Electr. Mach. Control.*, vol.15, pp. 74-76, 2011.

[2]　F. L. Fu, "Engineering calculation of the starting temperature rise for the asynchronous motor", *Electr. Machinery Technol.*, vol. 2, pp. 9-11, 1993.

[3]　J. D. Gao, X. H. Wang, and F. H. Li, *Analysis of AC Motor and its System*. Tsinghua University Press: Beijing, 2005.

[4]　M. J. Hary, and C. K Narayan, "Starting performance of saturated induction motors", in: IEEE Power Engineering Society General Meeting, June 24-28, Tampa, FL, 2007 , pp. 1-7.

[5]　E. F. Fuchs, M. Poloujadoff, and G. W. Neal, "Starting performance of saturable three-phase induction motors", *IEEE Trans. Energy Convers.*, vol.3, pp. 624-631, 1988.

[6]　D. W. Meng, Y. Y. Xia, and Y. Yang, "Calculation of starting characteristics for medium-sized motors with high-voltage in YKK series", *Electr. Mach. Control*, vol. 15, pp. 50-53, 2011.\

[7]　A. J. Zhang, "The research on the dynamic process of induction motors considering skewed rotor", Beijing: North China Electric Power University, 2006.

[8]　Z. W. Sheng, "Calculation of temperature rise of rotor bars and end rings of squirrel cage induction motors during starting", *Explosion-proof Electr. Mach.*, vol. 40, pp. 12-14, 2005.

[9]　Z. W. Shi, and C. Q. Xu, "Synthesis calculation of mixed ventilation and heat for large and medium induction motor", *Large Electr. Mach.*, no. 5, pp. 34-37, 1993.

[10]　W. L. Li, S. F. Li, and Y. Xie, "Stator-rotor coupled thermal field numerical calculation of induction motors and correlated factors sensitivity analysis", *Proceedings of the CSEE*, China, vol.27, pp. 85-91, 2007.

[11]　H. Y. Yan. "*Calculation and analysis of fluid flow and heat transfer in medium size high voltage asynchronous motor*", Master Thesis, Harbin: Harbin University of Science and Technology, 2011.

[12]　D. Z. Huang, "*Numerical calculation of electromagnetic fields and temperature fields of large and medium asynchronous motor*", Master Thesis, Harbin: Harbin University of Science and Technology, 2004.

[13]　Y.T Wei, and D. W. Meng, and J. B. Wen, *Heat Exchanges in the Motor*. China Machine Press: China, Beijing 1998.